and

$$2Q_iQ_r=-\frac{4\pi\omega}{c^2}\sigma_+''. \tag{17}$$

The conductivity on the right-hand side of Eqs. (16) and (17) is to be evaluated at the real part of the wave vector (i.e., at $Q=Q_r$) and these equations are strictly valid only when $Q_r\gg Q_i$ since otherwise the helicon propagation cannot be accurately described by a complex wave vector. Since in the region $H>H_D$ we have $\sigma_+''\gg\sigma_+'$, then from Eqs. (16) and (17) we get $Q_r\gg Q_i$, i.e., the helicon wave is only slightly damped within a wavelength. The helicon damping observed by Grimes and Libchaber[7] does show this characteristic property ($Q_r\gg Q_i$) of $\Delta n=0$ transitions.

The large quantum oscillations in σ_+' give rise in general to oscillations in both the wavelength ($2\pi Q_r^{-1}$) and the attenuation (Q_i) of the helicon wave in accordance with Eqs. (16) and (17). However, since $\sigma_+''\gg\sigma_+'$ we obtain from Eqs. (16) and (17)

$$\frac{\Delta Q_r}{Q_r}\approx-\frac{1}{2}\frac{\Delta\sigma_+''}{\sigma_+''};\quad \frac{\Delta Q_i}{Q_i}\approx\frac{\Delta\sigma_+'}{\sigma_+'}-\frac{1}{2}\frac{\Delta\sigma_+''}{\sigma_+''}. \tag{18}$$

Since large Q.O. occur only in the real part of the conductivity[10,11] (σ_+'), we see from Eq. (18) that the Q.O. in the attenuation will be much larger than those in the wavelength.

In the alkali metals the Fermi surface is nearly spherical so that no tilted orbits are present. Thus on the basis of the model of tilted-orbit effects discussed we expect no quantum oscillations when $H>H_D$. Grimes and Libchaber have observed Q.O. in potassium with $H>H_D$.[6,7] However, the oscillations are much smaller in magnitude than those observed in other metals. Thus their observations in potassium are in agreement with the model of tilted-orbit effects and the small Q.O. which they do detect may perhaps be due to a small spin-orbit coupling.

Quantum oscillations of large magnitude have been observed in Al.[6,7] From the observed period of the oscillations, the orbits of the Fermi surface which give rise to the Q.O. have been identified as tilted orbits in real space. It thus appears that the observations in Al are directly related to the tilted-orbit effect.

We would like to thank Dr. C. C. Grimes and Dr. A. Libchaber for kindly making their results available to us prior to publication and for several helpful discussions of these topics.

PHYSICAL REVIEW VOLUME 161, NUMBER 3 15 SEPTEMBER 1967

Optical Absorption by Excitons in Amorphous Selenium

K. J. SIEMSEN AND E. W. FENTON
Noranda Research Centre, Pointe Claire, Quebec, Canada
(Received 20 March 1967)

Evidence is presented in support of a postulate proposed by Hartke and Regensburger in 1965, that the absorption edge in amorphous selenium is dominated at room temperature by an exciton band. Measurements of the temperature shift of the absorption edge show that the temperature shift decreases rapidly as the absorption increases, reaching negligible values well before the maximum absorption is reached. Photoconductive and nonphotoconductive components of the absorption are resolved on the basis of quantum efficiency. The nonphotoconductive or exciton component of absorption is related to vibrational frequencies of the short-range atomic order.

INTRODUCTION

MEASUREMENTS of the spectral response of photoconductivity in amorphous selenium[1–4] have shown that the quantum efficiency (number of free carriers generated per absorbed photon) is near unity at wavelengths below $\sim0.5\,\mu$ in amorphous selenium. However, at longer wavelengths where the absorption is still strong, the quantum efficiency becomes small. Hartke and Regensburger[5] have measured separately the electron and hole quantum efficiencies. They postulate that a photoconductive component of the absorption is due to interband transitions (or some other model with photoconductive characteristics, since it has not been well established that amorphous selenium can be described by a band model). The nonphotoconductive part of the absorption is attributed to a separate mechanism with room-temperature characteristics remarkably similar to absorption by localized excitons in alkali halides.

Measurements will be presented in this discussion of optical absorption varying from 5×10^5 cm^{-1} to less than 1 cm^{-1}, at temperatures ranging from 77 to ~700°K, and in the wavelength range 0.4–10 μ. The absorption values agree (within a reasonably small experimental error) with other room-temperature measurements, and with temperature-dependent measurements confined to a more restricted wavelength and

[1] J. Dresner, J. Chem. Phys. **35**, 1628 (1961).
[2] M. A. Gilleo, J. Chem. Phys. **19**, 1291 (1951).
[3] P. H. Keck, J. Opt. Soc. Am. **42**, 221 (1952).
[4] R. A. Fotland, J. Appl. Phys. **31**, 1558 (1960).
[5] J. L. Hartke and P. J. Regensburger, Phys. Rev. **139**, A970 (1965).

absorption range.[2,6–14] The new results indicate that the temperature shift of the absorption edge is strongly dependent on the magnitude of the absorption, in agreement with previous indications, decreasing to very small or negligible shifts well below the absorption maximum. As we will discuss, this behavior lends strong support to the earlier evidence of Hartke and and Regensburger[5] that localized excitons contribute strongly to the absorption at the absorption edge. If temperature shifts of the absorption edge were related to interband transitions, or a similar mechanism, they would not decrease to negligible values as the magnitude of the absorption becomes large.

THEORY

For photon energies in regimes of strong absorption, and particularly when more than one absorption mechanism participates strongly, variation of the refractive index with photon energy must be considered as an integral part of the absorption theory.[15–17] The medium may be characterized by a single optical parameter, which is often the complex index of refraction, $N=n-ik$, where n is the ordinary index and k is the extinction coefficient. The absorption coefficient is related to k by $K=4\pi\nu k/c$, where c is the free space velocity of light and ν is the frequency. According to the well-established theory of optical absorption,[18] neither the absorption coefficients nor the refractive indices arising from several independent mechanisms are additive, although the products are additive (within limits):

$$Kn=\sum_i K_i n_i. \tag{1}$$

It has been stressed by Hartke and Regensburger that when more than one mechanism participates strongly in the absorption, the absorbing medium is most appropriately discussed in terms of the complex dielectric constant $\epsilon=\epsilon_1-i\epsilon_2$, comprised of the real and imaginary parts ϵ_1 and ϵ_2. ϵ_1 and ϵ_2 are related to the complex index of refraction by $\epsilon=N^2$, and

$$\epsilon_1=n^2-k^2,$$
$$\epsilon_2=2nk=(2\pi\nu)^{-1}cnK. \tag{2}$$

ϵ_1 and ϵ_2 are related by the well-known Kramers-Kronig dispersion relations,[19] and since $\epsilon_2=\sum_i \epsilon_2{}^i$ is additive, ϵ_1-1 is also additive. If either K or n is measured through the entire frequency spectrum, the other can be determined through Eq. (2) and the Kramers-Kronig relations. If both are measured through the entire frequency spectrum, consistency of the measurements can be checked.

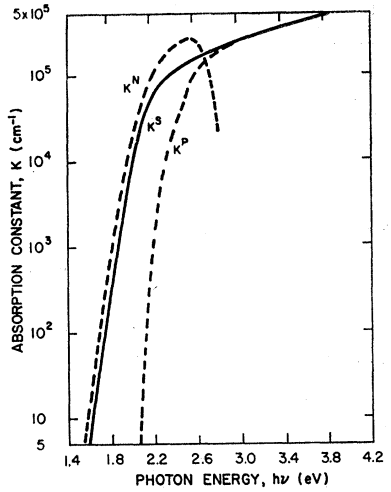

FIG. 1. Optical absorption in amorphous selenium at room temperature K^S, resolves into photoconductive and nonphotoconductive components K^P and K^N on the basis of quantum efficiency, from Ref. 5 (Fig. 6). Note that $K^S\neq K^P+K^N$.

Hartke and Regensburger have resolved the total absorption in amorphous selenium (at room temperature) into photoconductive and nonphotoconductive components, using the additivity of ϵ_2 and ϵ_1-1 and measurements of the quantum efficiency. (By definition, the quantum efficiency η is 1 for photoconductive processes and zero for nonphotoconductive processes.) Figure 6 of Ref. 5, reproduced in Fig. 1. illustrates that $K^S\neq K^P+K^N$. Here K^S is the total optical absorption, and K^P and K^N are the components due to photoconductive and nonphotoconductive processes. The nonphotoconductive absorption at slightly lower photon energies is suppressed and the photoconductive absorption at higher photon energies is enhanced when the two absorption processes are combined. This is because the photoconductive index of refraction n^P is greater than the ordinary index n^S, and the nonphotoconductive index n^N is less than n^S. The "exciton structure" of the absorption edge which usually distinguishes exciton absorption does not appear since n^N is considerably less than n^P.

The nonphotoconductive contribution to absorption can be analyzed in terms of phonon-broadened absorption due to localized excitons. Mahr[20] has extended the

[6] H. A. Gebbie and E. W. Saker, Proc. Phys. Soc. (London) **B64**, 360 (1951).
[7] J. J. Dowd, Proc. Phys. Soc. (London) **B64**, 783 (1951).
[8] J. Stuke, Z. Physik **134**, 194 (1953).
[9] C. Hilsum, Proc. Phys. Soc. (London) **B69**, 506 (1956).
[10] W. F. Koehler, F. K. Odenkrantz, and W. C. White, J. Opt. Soc. Am. **49**, 109 (1959).
[11] R. S. Caldwell and H. Y. Fan, Phys. Rev. **115**, 664 (1959).
[12] H. Gobrecht and A. Tausend, Z. Physik **161**, 205 (1961).
[13] W. Kamprath, Ann. Physik **9**, 382 (1962).
[14] W. Henrion, Phys. Status Solidi **12**, K113 (1965). Temperature-dependent measurements on selenium single crystals, $K<10^3$ cm^{-1}.
[15] J. J. Hopfield, Phys. Rev. **112**, 1555 (1958).
[16] D. L. Dexter, Phys. Rev. **101**, 52 (1956).
[17] S. I. Pekar, J. Phys. Chem. Solids **5**, 11 (1958).
[18] R. S. Knox, in *Solid State Physics*, edited by F. Seitz and D. Turnbull (Academic Press Inc., New York, 1963), Suppl. 5.
[19] P. Roman, *Advanced Quantum Theory* (Addison-Wesley Publishing Company, Reading, Massachusetts, 1965).
[20] H. Mahr, Phys. Rev. **132**, 1880 (1963).

theory derived by Toyozawa[21–23] for this mechanism. An expression is obtained for the shape of the exciton absorption curve which applies to both high- and low-absorption regimes, and intermediate regimes as well. The relative transition probability for absorption by localized excitons (strong exciton-lattice coupling) is given by

$$\epsilon_2{}^N(h\nu)^2 = A(T)\exp\{-\sigma(h\nu_0-h\nu)\} \times\int_\alpha^{+\infty}\frac{\exp(-x^2)}{(x-\alpha)^{1/2}}dx. \quad (3)$$

(This expression is slightly different from those in both Refs. 5 and 20. In the former, only a single tempertture was considered, and in the latter the denominator of the integrand was omitted.) $A(T)$ is a parameter determined by the maximum value of $\epsilon_2{}^N(h\nu)^2$. $\alpha=-\{\tau(h\nu_0-h\nu)-\sigma/2\tau\}$, and σ and τ are temperature-dependent parameters. This expression reduces to a Gaussian shape for the absorption band near maximum absorption, and to exponential dependence on photon energy when the absorption is much less (Urbach's rule).

The Toyozawa theory treats phonon broadening of exciton absorption in terms of linear exciton-lattice interactions near the absorption maximum. The shape of the transition probability is described by the limiting case of Eq. (3) in this regime (approximately)

$$\epsilon_2{}^N(h\nu)^2 \propto \exp\{-\tau^2(h\nu_0-h\nu)^2\}, \quad (4)$$

with

$$\tau^2=(\tau_0{}^2/kT)F(\omega_1),$$

where

$$F(\omega)=\frac{2kT}{\hbar\omega}\tanh\frac{\hbar\omega}{2kT}.$$

τ_0 is a constant of the solid. Toyozawa assumes that linear processes are dominated by longitudinal acoustic phonons, and thus ω_1 is an effective frequency which describes a suitable average over longitudinal acoustic modes.

When $K/K_{\max}\ll 1$, Toyozawa derives Urbach's rule assuming that quadratic exciton-lattice interactions are dominant, and he relates these to longitudinal optic modes (or transverse acoustic modes). In this case Eq. (3) reduces to

$$\epsilon^{2N}(h\nu)^2 \propto (h\nu_0-h\nu)^{-1/2}\exp\{-(\sigma+0.4016\tau)(h\nu_0-h\nu)\}, \quad (5)$$

$h\nu_0>h\nu$, and $\sigma=(\sigma_0/kT)F(\omega_2)$. Here σ_0 is a constant. $\hbar\omega_2$ is the energy of the longitudinal optical or transverse acoustic phonons. When there is more than one frequency of vibration contributing to the exciton-lattice interaction, ω_2 can be regarded as an effective frequency which describes some appropriate average.

[21] Y. Toyozawa, Progr. Theoret. Phys. (Kyoto) 22, 455 (1959).
[22] Y. Toyozawa, Progr. Theoret. Phys. (Kyoto) 20, 53 (1958).
[23] Y. Toyozawa, Progr. Theoret. Phys. (Kyoto) Suppl. 12, 111 (1959).

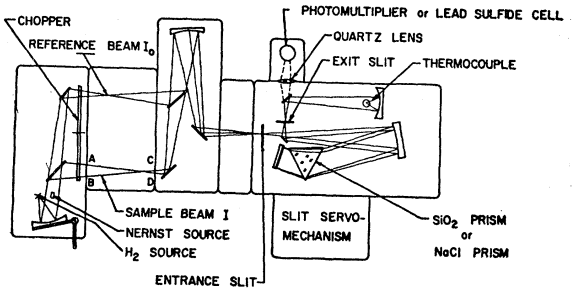

FIG. 2. Optical alignment of Perkin-Elmer 13U optical absorption apparatus.

Thus, experimentally observed shifts of the optical absorption edge due to phonon broadening of the exciton absorption band can be related to longitudinal optical and transverse or longitudinal acoustic modes of vibration of the lattice (or to vibrations of the short-range atomic order in the case of amorphous selenium, which can probably not be thus classified).

EXPERIMENTAL PROCEDURE

The optical absorption was measured with a Perkin-Elmer double-beam spectrometer (Model 13U), with an optical alignment as shown schematically in Fig. 2. The intensity ratio of the light beam (I) passing through the specimen to a reference beam (I_0) is measured by a phase sensitive amplifier. The spectrometer was calibrated in the wavelength range 0.31–1.97 μ using the emission lines of a high-pressure Hg lamp as a standard, and in the range 2.5–16 μ using absorption lines of a 0.05-mm-thick polystyrene film.

Measurements of the temperature dependence of the transmission and reflection of amorphous selenium above room temperature were made with the selenium confined between quartz or NaCl plates, and heated by electrical means. Temperature was monitored and controlled by thermocouples. A liquid-nitrogen cryostat was used for measurements from 77 to 273°K.

For measurements of reflectivity, the reference beam was reflected from either a silver or an aluminum mirror. The specimen beam was reflected from a polished selenium surface, or at high temperatures from a liquid selenium surface in contact with glass. Although standard precautions were taken in calibration of the spectrometer for reflectivity measurements as well as for transmission measurements, the reflectivity measurements were of lower accuracy and consistency. This is due primarily to the fact that the beam incident on the specimen is not plane parallel, so that small deviations of the specimens from flatness strongly influence reflectivity values.

All determinations of the absorption coefficient were made from transmission measurements, with transmission less than 10%. Reflectivity of window materials was compensated for in the calculations.

SPECIMEN PREPARATION

Specimens originated from commercial high-purity selenium (Canadian Copper Refiners Limited) subsequently vacuum distilled at a pressure of 10^{-4} Torr. A shift of the absorption edge and the absence of a weak absorption band at $\sim 11\ \mu$ occurs when compared with untreated selenium. (Distillation in high vacuum reduces the absorbed oxygen.)

Specimens in the thickness range 0.5–10 cm were prepared from quenched selenium distillation ampoules by cutting. Specimens of 0.05–0.5-cm thickness were prepared by pouring liquid selenium between NaCl or quartz plates, and then cooling the assembly with cool air. This technique is preferable to pressing liquid selenium between cool plates since formation of thin polycrystalline layers a few microns beneath the surface is prevented. Specimens prepared by the latter method may have a weak reflectivity band near $\lambda = 13.5\ \mu$.

Specimens in the thickness range 0.05–50 μ were prepared by vacuum evaporation onto thin quartz plates. Optical measurements were commenced immediately in this case, since crystallization occurs after only a few days at room temperature. Thickness of such thin films was determined both by weight and by Newton's visible light interference method.

EXPERIMENTAL RESULTS

The optical absorption in amorphous selenium as a function of both photon energy and temperature is shown in Fig. 3. Clearly the temperature shift of the absorption edge is not similar to temperature shifts in semiconductors such as Ge, since the shift is strongly dependent on absorption amplitude, decreasing to approximately zero well before the maximum absorp- This behavior cannot be explained by any of the well-known arguments relating temperature shifts to valence-band–conduction-band transitions, or to processes involving impurity states.[24]

Near the absorption maximum, where the temperature shift is negligible, the absorption at room temperature has been shown by Hartke and Regensburger to be almost entirely photoconductive. Thus we regard the temperature dependence of the photoconductive component of absorption as much less than that of the nonphotoconductive part dominant at lower photon energies. If the imaginary part of the dielectric constant for photoconductive absorption $\epsilon_2{}^P$ is regarded as constant with temperature, $\epsilon_2{}^P$ (25°C) determined in Ref. 5 can be used throughout the temperature range of the experiments to determine the nonphotoconductive component of the dielectric constant:

$$\epsilon_2{}^N(T) \simeq \epsilon_2{}^S(T) - \epsilon_2{}^P(25°\text{C}). \qquad (6)$$

(In any case, $\epsilon_2{}^P$ is much less than $\epsilon_2{}^N$ at the absorption edge when $K \ll K_{\max}$.) $\epsilon_2{}^S$ is determined using Eq. (2) and

[24] T. S. Moss, *Optical Properties of Semiconductors* (Butterworths Scientific Publications, Ltd., London, 1959).

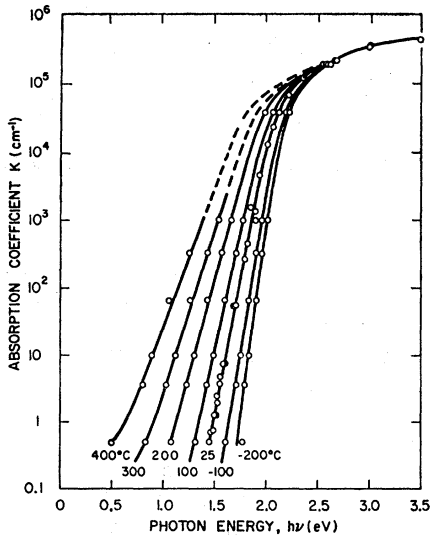

FIG. 3. Optical absorption of amorphous selenium at temperatures from −200 to 400°C. Points above $K = 2.5 \times 10^5$ cm^{-1} refer to −200 and 200°C and encompass experimental values not shown for intermediate temperatures.

the temperature-dependent refractive index.[2,10,11,25,26] Figure 4 shows the nonphotoconductive transition probability $\epsilon_2{}^N(h\nu)^2$ determined in this way, and compared with the transition probability for localized excitons of Eq. (3). Measurements of the refractive index are not yet sufficiently extensive or accurate at temperatures other than room temperature to warrant use of the Kramers-Kronig relations as a consistency check on absorption and refractive-index measurements. However, this does not restrict determination of $\epsilon_2{}^S(T)$ more than the accuracy of the absorption measurements.

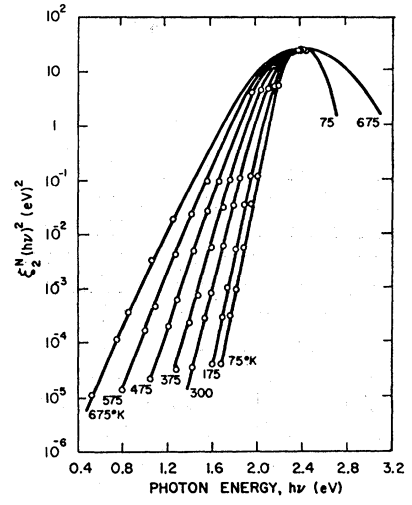

FIG. 4. Relative probability of nonphotoconductive transitions as fitted to Eq. (3). $h\nu_0 = 2.44$ eV, $\hbar\omega_1 = 1.3 \times 10^{-2}$ eV, $\hbar\omega_2 = 4.6 \times 10^{-2}$ eV.

[25] E. W. Saker, Proc. Phys. Soc. (London) **B65**, 785 (1952).

[26] K. Siemsen has measured n from 0.5 to 2 μ and at temperatures ranging from 77 to ~750°K, to be published when measurements are complete.

The fact that no "exciton structure" occurs on the absorption edges in Fig. 3 is attributed to differences between the refractive indices for photoconductive and nonphotoconductive absorption. The absorption coefficients are not additive (Fig. 1) and the exciton absorption peak is suppressed into the nonphotoconductive absorption edge.

DISCUSSION

There are two important features of the optical absorption in amorphous selenium according to our experimental results:

(1) The nonphotoconductive component is strongly temperature-dependent and arises from absorption by intrinsic excitons which are localized by strong exciton-lattice interactions. The experimental results agree closely with predictions of the theory developed by Toyozawa,[21–23] as shown in Fig. 4. Phonon energies corresponding to linear and quadratic exciton-lattice coupling are $\hbar\omega_1=1.3\times10^{-2}$ eV and $\hbar\omega_2=4.6\times10^{-2}$ eV, respectively. $\hbar\omega_2$ is accurate to $\sim5\%$; however, the error in $\hbar\omega_1$ may be as high as 30–40%, since $\hbar\omega_1$ is determined almost completely by only five data points near $\epsilon_2{}^N(h\nu)^2=5(\text{eV})^2$ (Fig. 4). In addition, each of these phonon energies is an effective energy for the exciton-lattice interaction which may be an appropriate average of several phonon energies.

Infrared absorption measurements show strong peaks attributed to vibrational modes of the short-range atomic order at $\sim3.2\times10^{-2}$ and $\sim6.1\times10^{-2}$ eV and a weak peak at $\sim4.6\times10^{-2}$ eV,[11,27,28] which would, of course, yield the effective phonon energy $\hbar\omega_2=4.6\times10^{-2}$ eV by a rough averaging. Infrared absorption peaks proximate to $\hbar\omega_1=1.3\times10^{-2}$ eV occur at $\sim1.2\times10^{-2}$ and $\sim1.5\times10^{-2}$ eV.[11,28] At the present time, modes of vibration corresponding to these infrared peaks have not been clearly identified. When this has been done it will be possible to determine which vibrational frequencies contribute to broadening of the exciton optical absorption, since $\hbar\omega_1$ is associated with linear exciton-lattice interactions, and $\hbar\omega_2$ with quadratic interactions. The energies $\hbar\omega_1$ and $\hbar\omega_2$ for amorphous selenium are similar to those determined for absorption by localized excitons in KCl, 1.6×10^{-2} and 6.0×10^{-2} eV.[20] The central photon energy of the intrinsic exciton absorption according to the theoretical curves which best fit experimental data, Fig. 4, is $h\nu_0=2.44$ eV. This value agrees closely with the value 2.45 eV determined by Hartke and Regensburger for absorption at room temperature.[5] (The difference is not significant.) These values for the intrinsic exciton ground-state level are separated by 0.08 and 0.09 eV from the conduction-band edge at 2.53 eV,[5] indicating an exciton reduced mass ~0.25 of the free-electron mass. If the electron and hole are of comparable mass, $m_e\sim m_h\sim0.5$. It should perhaps be emphasized that the values 0.08 and 0.09 are only accurate to a factor of 2 or 3, and that we can only say with confidence that m_e is of order unity or slightly less. m_e is much less than values such as 9 or 33 determined from drift mobility studies and by assuming that the temperature shift of the absorption edge is associated with changes of the energy gap[24] (which we regard as an incorrect procedure, since the photoconductive absorption appears to be relatively temperature-independent, as we have discussed). Measurements of the Faraday rotation in selenium indicate an effective mass $m\sim2.5$,[24] in much closer agreement with the determination from exciton absorption.

(2) The photoconductive component of the optical absorption appears to be only slightly temperature-dependent in comparison with the nonphotoconductive component. This could be more completely established by measurements of quantum efficiency using the pulse technique[5] at temperatures other than room temperature. At the present time, evidence consists of the absorption curve in the range $K=2.5\times10^5$ to 5×10^5 cm^{-1}, which is part of the photoconductive edge and is not temperature-dependent, and Fig. 4, which shows nonphotoconductive absorption compared to theory, assuming that photoconductive absorption is temperature-independent. (If the temperature dependence of photoconductive absorption were very great, agreement between theory and experiment in Fig. 4 would likely be much poorer.)

The temperature-expansion coefficient of amorphous selenium is large in comparison to Ge or Si ($\sim5\times10^{-5}$ per °C, linear). If the photoconductive absorption associated with transitions from nonconducting to conducting states is only slightly temperature-dependent, certain features of the electronic conduction model appropriate to amorphous selenium are indicated. It appears probable that within the rings or chains of the short-range atomic order, well-defined valence and conduction bands exist which are only slightly temperature-dependent. Most of the temperature expansion of amorphous selenium is probably associated with displacements of regions of short-range order with respect to each other, rather than to changes of the short-range order parameters. An appropriate conduction model would appear to be valence and conduction bands in regions of short-range order, and potential barriers separating such regions. In this case, drift mobilities and "space-charge-limited currents"[29] can be associated with tunneling through potential barriers.

ACKNOWLEDGMENTS

The authors are grateful to C. H. Griffiths, F. Rosenblum, and H. Sang, who assisted with specimen preparations, and to Dr. C. H. Champness, for discussions regarding experimental procedure. The experiments were jointly supported by Canadian Copper Refiners Limited and a Defence Research Board of Canada industrial research grant.

[27] A. Vasko, Czech. J. Phys. **B13**, 827 (1963); **1.15**, 170 (1965).
[28] G. Lucovsky, A. Mooradian, W. Taylor, G. B. Wright, and R. C. Keezer, Solid State Commun. **5**, 113 (1967).
[29] J. L. Hartke, Phys. Rev. **130**, 134 (1963).